3D MONTE CARLO SIMULATION OF PHASE SEPARATION IN A BINARY ALLOY

A.S. SHIRINYAN, YU.S. BELOGORODSKY

B. Khmelnytskyi Cherkasy National University, Faculty of Physics
(81, Shevchenko Str., Cherkasy 18031, Ukraine; e-mail: shirinyan@phys.cdu.edu.ua)

UDC 539.3

The kinetics of new phase nucleation in a binary alloy with the fcc crystal lattice has been analyzed in detail making use of the three-dimensional Monte Carlo simulation. The dependences of various parameters of the process — the average dimension of new-phase particles, number and volume of new-phase clusters, distribution function of particles over their dimensions, dispersion, and supersaturation — on time and the parameters of the system have been calculated. The approximation proposed considerably improves our understanding of the mechanisms of nucleation and growth of the new-phase particles in a metastable nanosystem.

1. Introduction

The greatest progress achieved during last decades in the fields of physical materials science and solid state physics is connected with the creation and use of micro- and nanostructured materials and systems — such as, e.g., bulk nanocrystalline alloys, microcircuits, and microchips — the operational characteristics of which are determined at a microscopic level. If dealing with such scales, the initial stages of the new phase appearance (nucleation) which result in macroscopic effects should be consider at a microscopic level.

Last years, a new technologically important class of materials — bulk nanocrystalline alloys which are a result of the incomplete decomposition of metastable amorphous multicomponent alloys — has been obtained [1, 2]. These metallic alloys (metallic glasses) can be applied as constructional materials in the aviation and space industry owing to their ability to hamper flawing. However, the processes of metallic glass formation and how this glass transforms into a nanocrystal are not clear enough yet.

In a bulk supersaturated system, the phase transition of the first kind (in our case, the phase separation) occurs through the nucleation and the growth of particles of a new phase. In experimental studies, four consecutive stages are distinguished: 1) nucleation, 2) the stage of independent growth of nuclei, 3) the intermediate or the so-called interim stage, and 4) coalescence and coagulation (or the so-called Oswald ripening stage) [3–8].

In the case of the decomposition of a supersaturated nanoalloy, the analytical analysis of all the stages of the system evolution becomes complicated by the circumstance that the conditions in the medium are ever-changing; namely, the supersaturation tends to zero, and the nucleation barrier enlarges to infinity [3, 4, 8]. Therefore, the appearance of new fluctuation-induced nuclei is practically impossible at the late stage of the phase decomposition process. In this case, nuclei, whose dimensions were supercritical under initial conditions, can become subcritical, so that their dissolution may start (coalescence). From this viewpoint, the final stage of phase separation is described by the Lifshits—Slezov—Wagner (LSW) theory of coalescence. Coalescence is calculated in the mean-field approximation and for infinitesimally small initial supersaturations, while the volume of the alloy is supposed infinitely large [5, 8]. At the same time, the problem of description of the initial decomposition stages (in micro- and nanoalloys, as well as in macrosystems) remains unresolved.

The vast majority of modern approaches are only capable to indicate the tendencies at the initial stage of reaction diffusion rather than to describe the process itself. Therefore, the task of the creation of such a computer model, which could reveal the features of the

new phase nucleation at the initial stages and trace the evolution of the system parameters in detail at every stage of the phase separation process, is topical.

Experimental methods for studying the phase separation in alloys can be complicated and expensive; this is why the computer simulation of this phenomenon is rather promising. In particular, such a high-speed method as the Monte Carlo (MC) one, allows the sufficient statistics for model nano-, micro-, and mesosystems that contain about 10^6 atoms to be collected within a reasonable time of the computer experiment. The corresponding MC researches have allowed the authors of works [9, 10] to simulate the evolution of such integral parameters as the order parameter, the temporal dependence of the new phase volume, and the average dimension of new-phase clusters.

In the majority of the previous works on the topic concerned, their authors considered a two-dimensional model, a simple cubic lattice, and a small number of atoms in the system [11–13]. The results obtained cannot be extrapolated to the case of real crystals. Moreover, the selected characteristics of the models did not enable the statistical treatment to be carried out, the distribution function of nuclei in the new phase to be constructed, and the evolution of the new phase to be studied both at the beginning and at the further stages of the decomposition process.

Having all that in mind, we attempted, in this work, to describe the definite stage of the phase transition of the first kind — namely, the process of phase formation at the initial stage of the reaction diffusion — at the atomic level by applying the three-dimensional (3D) computer simulation of the crystalline nanoalloy. We have constructed a kinetic MC model for the phase decomposition in a binary system with the fcc lattice and analyzed the alloy decomposition at every evolution stage of the system concerned. For this purpose, two following tasks of the research had to be tackled:

— an MC computer model for the microscopic description of phase transitions in a supersaturated alloy had to be created, and

— a computer simulation of the kinetics of nucleation and growth of the new phase in the course of the phase separation in the binary alloy had to be carried out.

Our research aimed at studying the first order phase transformations in a binary system and the process of phase formation. The subjects of the research were the decomposition kinetics at every stage and the behavior of the characteristic parameters of the system in the course of phase separation. The method applied for studying the kinetics of system relaxation was the method of MC computer simulation of the vacancy diffusion. We extensively used the programming languages Borland Pascal and Borland Delphi 7.0 for the creation of the computer code, the system of computer mathematics Waterloo Maple 9.0 for visualizing 3D images, and the software package Golden Software Grapher 2.0 for the graphic analysis.

Such an approach allowed us to study, "*in situ*", the reaction diffusion in a supersaturated binary alloy with the fcc lattice. If the alloy is first heated up to a high temperature, which corresponds to a homogeneous solid solution of component B in component A, and then quickly quenched to a temperature below the temperature of phase formation, a metastable state of the solution can be obtained. This nonequilibrium single-phase state can change to the equilibrium two-phase one by means of separating — namely, nucleating — a new phase [14]. The time interval of such a transition would depend on the initial supersaturation level of the solution. Such a supersaturated solid solution served for the initial state in the simulation procedure.

2. Monte Carlo Simulation of the Phase Separation Process in a Binary Alloy

2.1. Monte Carlo method

The MC method is based on a random choice among the eligible trajectories of the system in the configurational phase space.

The first approximation of this method was described in 1949 in the article by Metropolis and Ulam. In 1953, a general algorithm for the canonical ensemble was proposed [12]. It includes the following steps:

1) a portion of the system is selected randomly, and the random trial variation of its coordinates is carried out;

2) the corresponding variation ΔE of the system energy is calculated;

3) if $\Delta E \leq 0$, the new configuration becomes accepted; otherwise, a random number R from 0 to 1 is generated;

4) if $R < \exp\left(-\frac{\Delta E}{kT}\right)$, the new configuration is accepted; if $R > \exp\left(-\frac{\Delta E}{kT}\right)$, the new configuration is rejected;

5) the next iteration is carried out starting from step 1.

For the further analysis, we should apply the fundamental concepts of the microscopic theory of diffusion in alloys and select a basic model of the metallic atom diffusion.

Various mechanisms of the atomic motion in the crystal — simple (motions over the interstitial sites, the vacancy mechanism of diffusion, mutual rearrangement

of neighbor atoms) and complicated ones (cyclic rearrangement of several atoms along some contour, the shift of an atomic chain, mechanisms involving the displacement of double and triple vacancies, and so on) — are considered in the theory [15–20]. We confine ourselves to the vacancy mechanism of diffusion only, which is the most probable case for metallic alloys.

2.2. Basic model of the vacancy diffusion

Below, we describe the model and the algorithm of the MC routine, which were used in the researches.

In order to calculate the configurational energy of the system, in which atoms were located at the lattice points, we used the Ising Hamiltonian, which took into account the energies of pair interatomic interactions only within the limits of the first coordination sphere [12, 21, 22]. A single vacancy was introduced into a spatial specimen with the fcc symmetry; the energy of interaction between this vacancy and other atoms was supposed zero [23]. The pair interaction potential Φ_{XY}, where the subscripts X and Y can accept one of the values A (for atoms A), B (for atoms B), or V (for vacancies), was assigned to every pair of the particles. In this case, the configurational energy of the whole system looks like

$$E = \frac{1}{2}\sum_{i=1}^{N_0}\sum_{j=1}^{Z}\Phi_{X_iY_j}, \tag{1}$$

where the external summation is carried out over all N_0 lattice points of the system, while the internal one only over the points within the first coordination sphere of the i-th lattice point.

In what follows, we use the modification of the MC method, the so-called residence time algorithm [10, 12]. This algorithm "forces" the vacancy to jump, and the direction of its displacement is selected according to the probability

$$p_i = \frac{\nu_i}{\sum\limits_{j=1}^{Z}\nu_j}, \tag{2}$$

where ν_i is the frequency of the atom-vacancy interchange in the i-th direction, and Z is the number of neighbor atoms. The total duration of the process is measured in MC-step (MCS) units and, in fact, coincides with the number of vacancy jumps.

The expression for the interchange frequency between the i-th atom and a vacancy (the vacancy jumps) in the first coordination sphere was taken in the form

$$\nu_i = \nu_{0i}e^{-Q_i/(kT)}, \tag{3}$$

where Q_i is the activation barrier height for the jump towards the i-th direction. The amplitude of Q_i depends on the sort of a diffusing atom and the dynamic characteristics of the crystal lattice (see below).

Provided that the first coordination sphere around the vacancy includes Z neighbor atoms, which are capable to make a jump, the probability p_i of the event that just the i-th neighbor atom would be engaged is proportional to ν_i (Eq. (3)) and determined by expression (2). This is the probability of the event that, of all the neighbor atoms, just the i-th one would appear at the vacant point in the next configuration, and the vacancy would occupy its place. (The probabilities are normalized to unity.)

Although the value of ν_{0i} can vary depending on the configuration, this dependence was neglected in calculations. We admitted only the dependence of the quantity ν_{0i} on the kind of the diffusing atom, by introducing two constants ν_{0A} and ν_{0B} (which might be equal to each other) for the corresponding atoms.

Consider a metal with a vacancy at one of the crystal lattice points. This vacancy is surrounded by Z neighbor atoms possessing the identical probabilities of the replacement by the vacancy. The quantity Z is the coordination number of the lattice ($Z = 8$ for the bcc lattice and 12 for the fcc and hcp one). Suppose that one of the neighbor atoms moves towards the vacancy, while all the rest atoms remain immovable at their lattice positions. In this case, the potential energy of such an atom would change with a distance, in the way shown in Fig. 1. This means that these two lattice points, where the potential energy is minimal, are separated from each other by a potential barrier, the top of which lies between them.

To calculate the energy Q_i, we used the model, where
— the energies of the start and end positions of the atom in the lattice are different, while the height E_0 of the potential relief is the same for all the atoms, and
— the depth of the well, where the atom is located, depends on its nearest environment (Fig. 1).

The barrier height for the atom which jumps from position 1 into position 2 was calculated by the formula $Q_1 = E_0 - E_1$, where E_0 is a unique constant for atoms of all kinds (its meaning is explained in Fig. 1), and E_1 is the energy of the atom in position 1.

The value of E_i for the i-th atom can be determined through the pair interaction potentials within the first

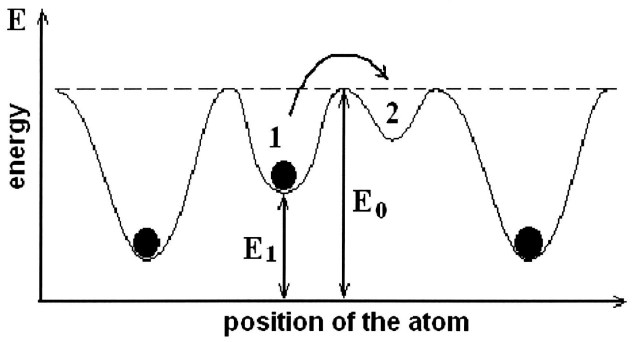

Fig. 1. Sketch of the barrier for the atom jumping from position *1* into position *2*. The barrier height is calculated by the formula $Q = E_0 - E_1$

coordination sphere by the formula

$$E_i = \sum_{j=1}^{Z} \Phi_{X_i Y_j}. \tag{4}$$

If this atom adjoins the vacancy, the barrier for his jump is

$$Q_i = E_0 - E_i. \tag{5}$$

While substituting formulas (3) and (5) into Eq. (2), the constant E_0 can be taken outside the exponent, so that it can be ultimately cancelled. Then, the expression for the probability looks like

$$p_i = \frac{\nu_{0i} e^{E_i/(kT)}}{\sum\limits_{j=1}^{Z} \nu_{0i} e^{E_i/(kT)}}. \tag{6}$$

Therefore, the algorithm for simulating the vacancy diffusion is as follows:

(i) The initial configuration of atoms is selected. The concentration of atoms is C_0, and they are rigidly fixed at the points of the regular fcc crystal lattice, being randomly distributed over the latter.

(ii) A vacancy is inserted (one of the fcc lattice points is designated as non-occupied).

(iii) For the given vacancy position, probabilities (6) are evaluated for all possible jumps by calculating energies (1) and (4). Afterwards, according to the probabilities found, the direction of the jump is selected randomly, by generating a random number R, and the interchange of the vacancy and the atom is carried out.

2.3. Basic characteristics

We propose a new approach to study the decomposition process at phase transitions of the first kind, which is based on the computer model of the vacancy diffusion described above. In the framework of this approach, we investigated the equilibrium states of the binary alloy. The results obtained were used for plotting the dependence of the concentration on time and the distribution function of clusters over their dimension $f(r)$, i.e. the number of nuclei with the size r. The model allows such most important characteristics of the distribution function as the average size (radius) $\langle r \rangle$ and the number N of the clusters, the dispersion Dr, the slope Sk, and the peak sharpness Kr to be calculated, provided that the MCS number and the initial concentration C_0 are fixed, using the relevant formulas

$$\mathrm{Dr} = \sqrt{\frac{\sum\limits_{n=1}^{n=N} (r_n - \langle r \rangle)^2}{N}}, \quad \mathrm{Sk} = \frac{\sum\limits_{n=1}^{n=N} (r_n - \langle r \rangle)^3}{N\,(Dr)^3},$$

$$\mathrm{Kr} = \frac{\sqrt{\sum\limits_{n=1}^{n=N} (r_n - \langle r \rangle)^4}}{N\,(Dr)^4} - 3, \quad \langle r \rangle = \frac{\sum\limits_{n=1}^{n=N} \sqrt[3]{N_n}}{N}.$$

Here, $N \equiv N(t)$ is the time-dependent number of clusters of the new phase, N_n is the number of atoms in the n-the cluster ($n = 1 \ldots N$), and the size r_n is defined as $r_n = \sqrt[3]{N_n}$.

The results obtained for the function $f(r)$ will also be compared in the space of average quantities, where the role of the parameter is played by the ratio between the new phase particle radius $r(t)$ and the average radius $\langle r \rangle$ rather than the radius r itself. The ratio $u = r/\langle r \rangle$ is a normalized dimension, which we introduce, in fact, in order to carry on a comparative analysis of our results with those of the well-known LSW theory [5, 8]. The average volume of the particles in the new phase is determined by the formula $\langle V \rangle = N^{-1} \sum_{n=1}^{N} N_n$, and the total volume of the new phase by the formula $V_{\mathrm{tot}} = \sum_{n=1}^{N} N_n$, so that the volume fraction of the new phase is $\rho = V_{\mathrm{tot}}/N_0$. The dispersion D, the slope Sk, and the peak sharpness Kr of the function $f(u)$ are determined by the formulas

$$D = \sqrt{\frac{\sum\limits_{n=1}^{N(t)} (u_n - 1)^2}{N(t)}}, \quad \mathrm{Sk} = \frac{\sum\limits_{n=1}^{N(t)} (u_n - 1)^3}{N(t)\,D^3},$$

$$\mathrm{Kr} = \frac{\sum\limits_{n=1}^{N(t)} (u_n - 1)^4}{N(t)\, D^4} - 3.$$

Here, $\bar{u} = 1$. (The magnitudes of Sk, as well as of Kr, in the usual space and in the space of average quantities coincide.)

In the following analysis, only those particles, in which one atom B was surrounded by not less than $N_{\min} = 10$ atoms of the same sort, were attributed to the new phase. Such a choice of the minimal number of surrounding atoms $N_{\min}$ was relative. In our case, the given value for $N_{\min}$ was caused by the alloy model with the fcc crystal lattice, where $Z = 12$. (The kinetics of phase separation in the cases, where $N_{\min} = 5$, 13, or 20, was considered separately.)

We also determined the running supersaturation in the alloy during the phase separation process as the function of the MCS. For this purpose, we had to know the concentration of component B outside the particles of the new phase, i.e. in that portion of the alloy, where there were no nuclei of the new phase. Below, we use the notation C for this concentration.

2.4. Simulation algorithm

Hence, the algorithm of the numerical method is as follows:

1) the size of the system N_0 and its initial configuration — the thermodynamic parameters and the initial concentration of the supersaturated alloy C_0 — is set by selecting the positions of atoms randomly in space;
2) the values of the quantities N, r_n, Dr, D, Sk, Kr, C, $f(r)$, $f(u)$, ρ, and E at $t = 0$ are determined;
3) the MC method described above is applied for simulating the vacancy diffusion within the time interval of the MCS;
4) new values of the characteristics listed in item 2 are determined at a new moment corresponding to the MCS.

2.5. Model of a metastable alloy

In our opinion, the proposed kinetic model of the reaction diffusion is adequate to the model of a regular solid solution, because the former takes into consideration the influence of the interatomic interaction only in the first coordination sphere. Following the theory of a regular solid solution, the metastable state of a binary alloy can be studied making use of the stability and decomposition criteria. From this standpoint, it is easy to construct a decaying metastable alloy. For this purpose, the energies of pair interaction Φ_{AA} and Φ_{BB} should be set so that the energy of ordering or the energy of mixing $E_{\mathrm{mix}} = 0.5(\Phi_{AA} + \Phi_{BB}) - \Phi_{AB}$ be negative (the alloy which tends to decay). Therefore, the pair interaction energies $\Phi_{AA} = \Phi_{BB} = -2 \times 10^{-20}$ J and $\Phi_{AB} = -1.8 \times 10^{-20}$ J at the temperature $T = 300$ K were adopted.

The analysis of the first and the second derivative of the Gibbs potential density (the energy per atom) for the simplified model of a regular solution testifies to that the alloy with the selected parameters is metastable within the concentration intervals $0.003 < C_0 < 0.1$ and $0.9 < C_0 < 0.997$, and absolutely unstable if $0.1 < C < 0.9$.

3. Kinetics of New Phase Nucleation and Phase Separation. Results and Discussion

Computer experiments were carried out for the fcc crystal lattice composed of 250 thousand, 500 thousand or 1 million atoms (the spatial analogs of the $100\times50\times50$, $100\times100\times50$, or $100\times100\times100$ lattice, respectively). The results obtained for the case with 500 thousand atoms will be reported below as an example. The periodic Born– Karman boundary conditions were applied along all the axes. The model parameters were the temperature $T = 300$ K, the pair interaction energies $\Phi_{AA} = \Phi_{BB} = -2\times10^{-20}$ J and $\Phi_{AB} = -1.8\times10^{-20}$ J, and the component mobilities (jump frequencies) $\nu_{0A} = 1 \times 10^{13}$ Hz and $\nu_{0B} = 3 \times 10^{13}$ Hz.

Fifty independent experiments were carried out. In order to study the thermodynamic properties of the ordered alloy, about 10^{10} MCSs were generated in every experiment.

Below, we report the basic results of computer experiments concerning the phase separation in a supersaturated binary alloy. The behavior of the function $f(u)$ can essentially vary depending on the initial supersaturation value. As a matter of fact, the cases of low and high initial supersaturations C_0 may be conventionally distinguished.

The evolution of the distribution function $f(u)$ at all the stages of decomposition is presented in Figs. 2 and 3. Here, only those particles were considered as the particles of the new phase with minimal dimensions, which were composed of not less than 10 atoms ($N_{\min} = 10$) of the sort B only. One can see that the unimodal distribution function, in the case of low initial supersaturation, first quickly becomes exponential (Fig. 2,*a*) and, afterwards, bimodal (Figs. 2,*b*–*e*). At the final stage, the distribution function becomes unimodal

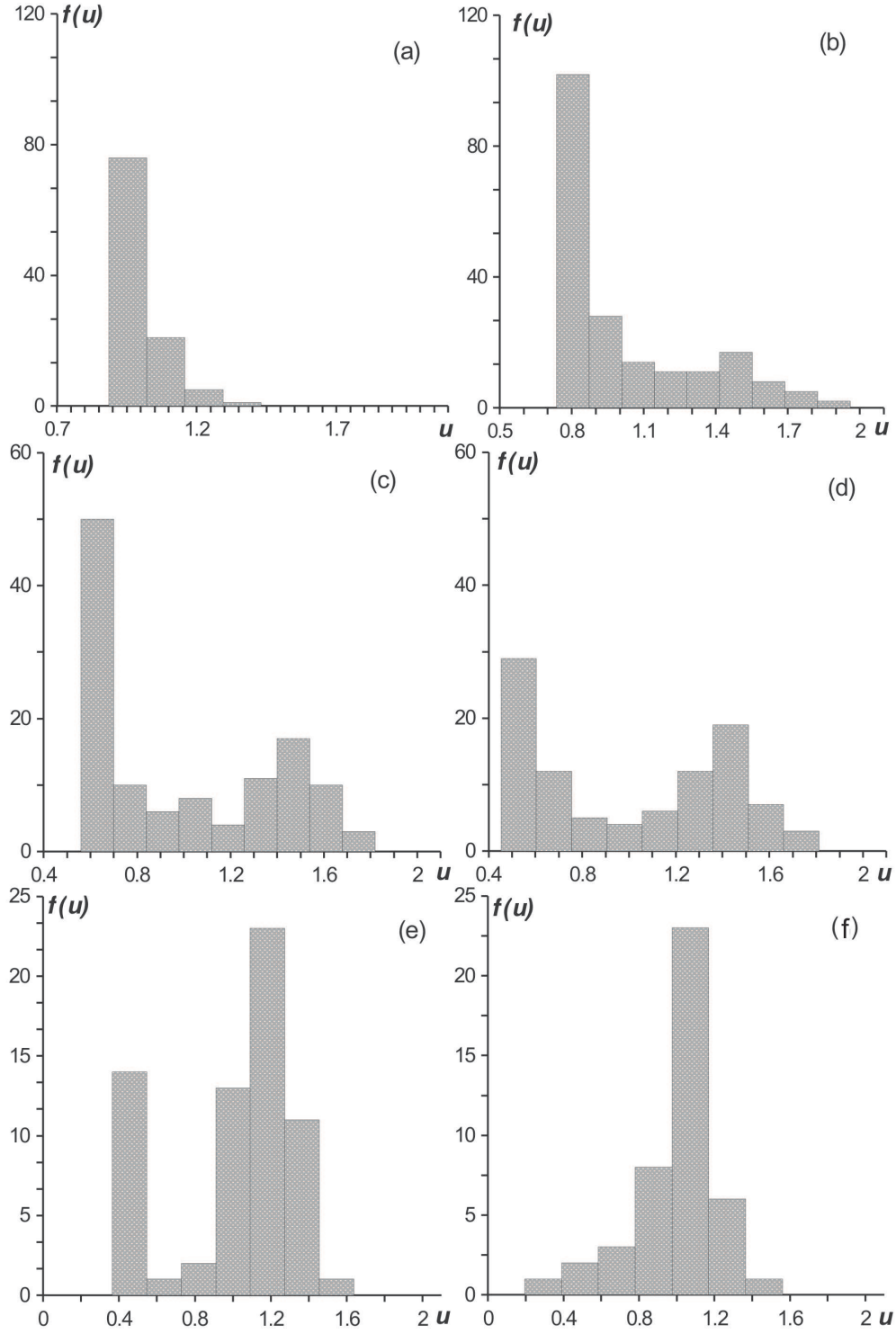

Fig. 2. Evolution of the distribution function of new-phase particles over their dimensions from the initial nucleation stage till the final stage of phase separation (coalescence) at a low initial supersaturation $C_0 = 0.05$ and at various numbers of MCSs: 0 (a, the initial distribution), 9.4×10^8 (b), 1.5×10^9 (c), 2.2×10^9 (d), 3×10^9 (e), and 5.4×10^8 (f)

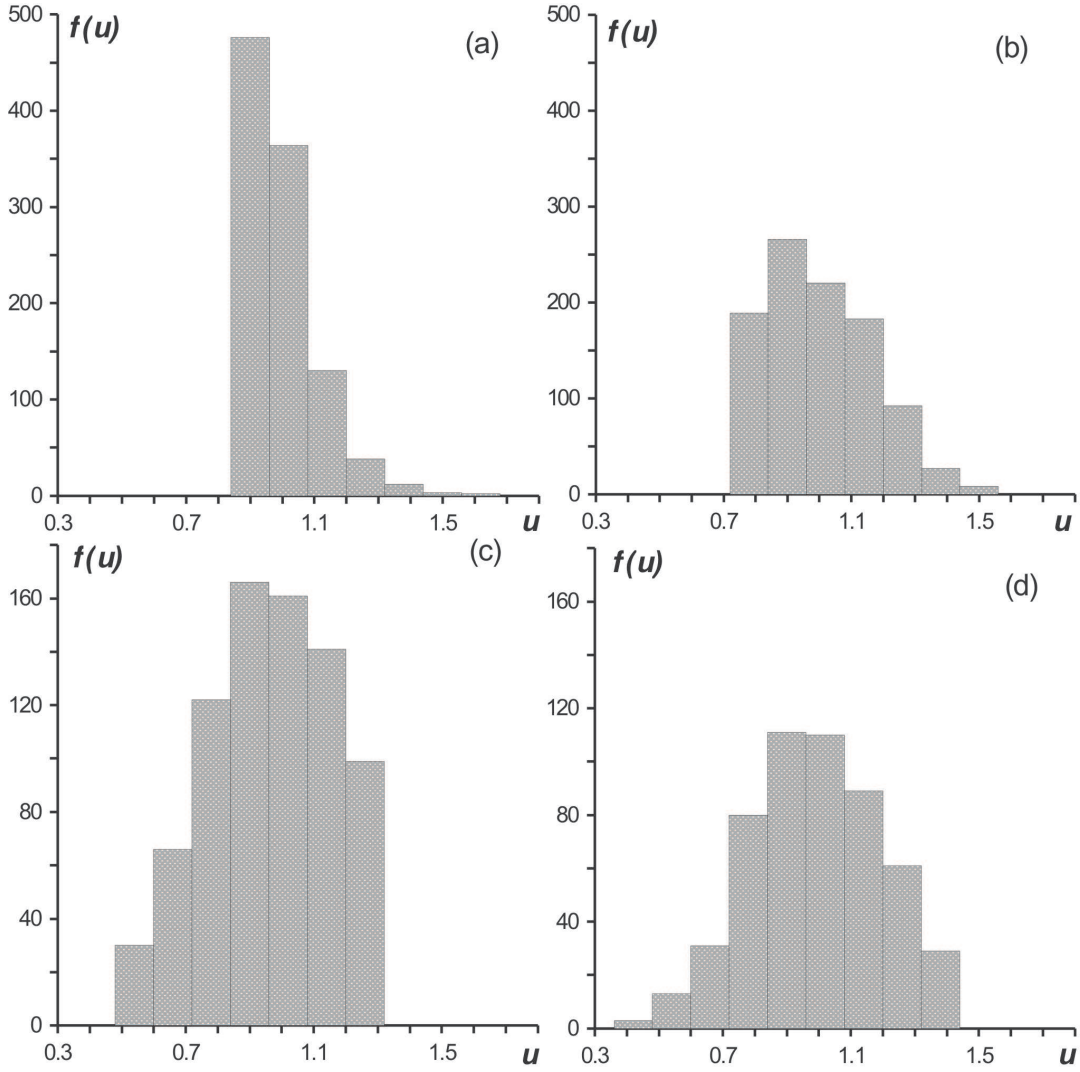

Fig. 3. The same as in Fig. 2, but at a high $C_0 = 0.1$. The numbers of MCSs are 0 (a, the initial distribution), 1×10^8 (b), 2×10^8 (c), and 4×10^8 (d)

again (Fig. 2,f). At low initial supersaturation values, this process looks like a "flowing" from one maximum to the other. Such a "flowing" process corresponds to the stage of independent growth and the interim stage [3,4].

At high initial supersaturation values, the behavior of the distribution function differs drastically. Namely, the distribution function remains unimodal, and its maximum moves towards larger dimensions (Figs. 3,a—d).

The results obtained demonstrate the characteristic features of the system evolution. These include the opportunity of a three-stage decomposition process in a binary alloy at low initial supersaturation values (nucleation, slow growth, and coalescence) and a two-stage decomposition at large initial supersaturation values (first, the appearance and the quick growth of the new phase occur simultaneously; afterwards, the slow coalescence and coagulation take place also simultaneously). The reduction of C_0 results in slowing down the whole process of phase separation.

Let us consider the process of decomposition in more details. The first stage is the nucleation.

3.1. Nucleation

At this stage, nano-, meso-, and macroparticles of the new phase arise. The model allows the emergence of the new phase to be traced for various initial conditions.

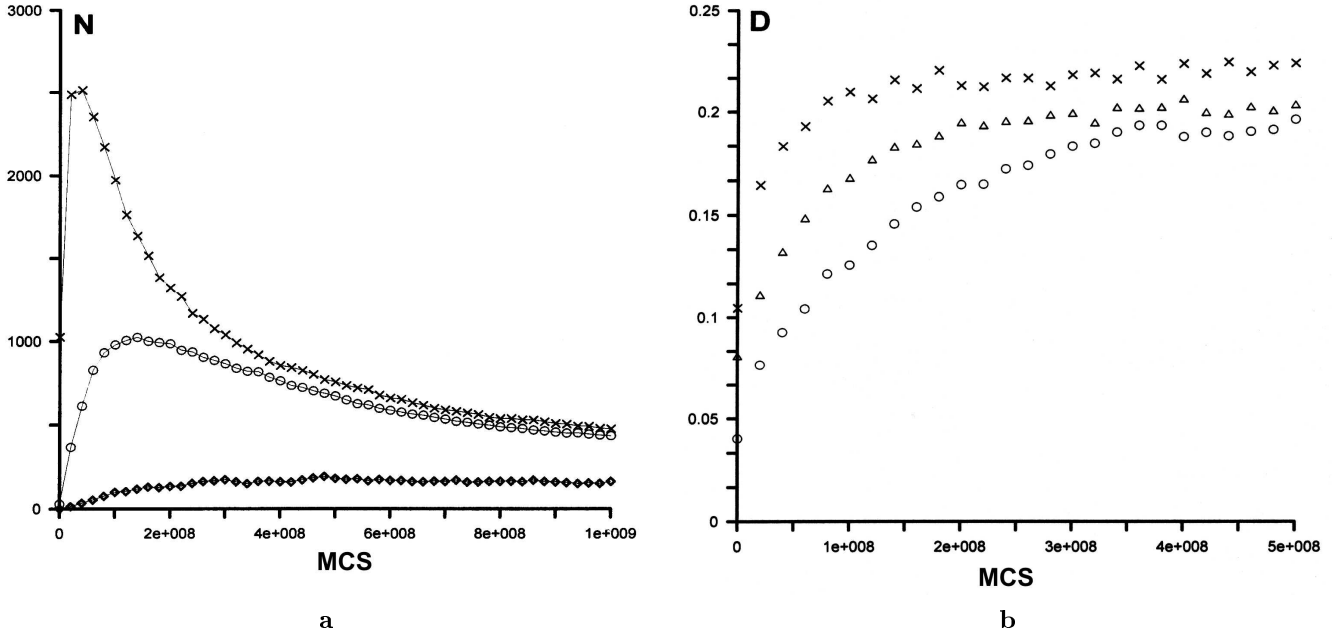

a b

Fig. 4. Number of new-phase particles N (a) and the dispersion D (b) as the functions of the MCS number for various initial values of $C_0 = 0.1$ (×), 0.075 (△), 0.05 (○), and 0.025 (◇)

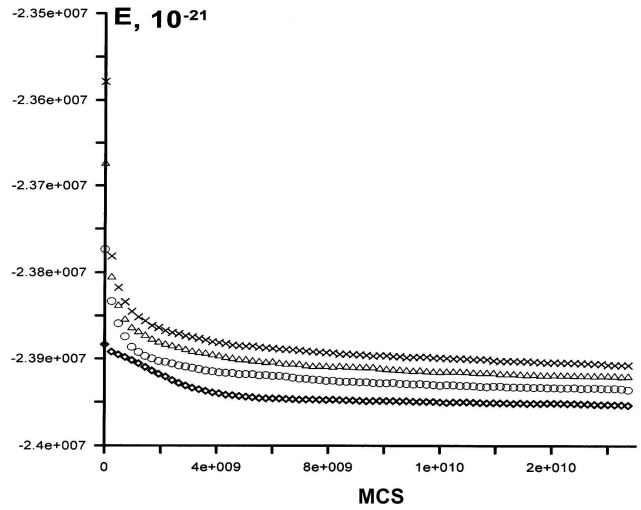

Fig. 5. Temporal dependences of the energy of the whole system for various initial values of C_0. The notations are the same as in Fig. 4. The decrease of the initial supersaturation results in the increase of the nucleation and growth times

The relevant dependences of the new-phase particle number and the particle dimension dispersion on the MCS number are depicted in Fig. 4.

In accordance with the model, the initial concentration C_0 was selected randomly, and the phase separation began as the particle dimension dispersion increased (Fig. 4,b).

Figure 4,a demonstrates that the reduction of initial supersaturation brought about the appearance of maxima in the evolution plots $N(t)$. The maximum point, which corresponded to the maximal number of the new-phase particles, became shifted towards larger times. The appearance of the maximum testified to that the process of new phase nucleation took place. The model made it possible to check the number of nuclei and their dimensions visually, with the help of the Maple 9.0 program (see below). For the description of the initial stage to be complete, the evolution of the distribution function dispersion for various values of C_0 is shown (Fig. 4,b).

3.2. Evolution of the basic characteristics

Depending on the initial supersaturation C_0, the shapes of the dependences $E(t)$, $\rho(t)$, $\langle V \rangle (t)$, $\langle r \rangle (t)$, $N(t)$, and $C(t)$ also changed. For large supersaturation values, the two-stage process of phase separation in the alloy was observed, when, right after the fast (short by time) nucleation, there occurred a quick transition to the stage of coalescence and coagulation. In fact, the stage of the independent growth of new-phase nuclei and the intermediate stage disappear [3–8]. Such a conclusion can be drawn while comparing Figs. 3—7. It is also confirmed by visual observations. As the magnitude of C_0 decreased, a gradual increase of the nucleation and

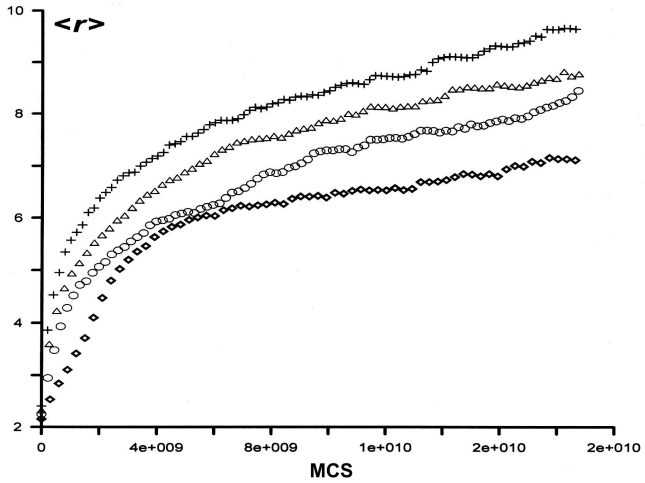

Fig. 6. The same as in Fig. 5, but for the evolution of the average dimension $\langle r \rangle$ of new-phase particles

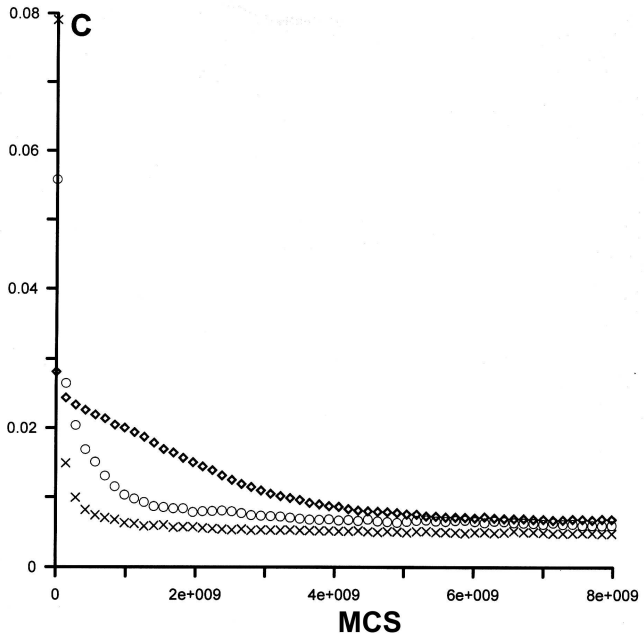

Fig. 7. Dependences of the concentration in the parent phase on time in the course of the decomposition. The notations are the same as in Fig. 4

growth times was observed (see a shift of the maximum in the dependence $N(t)$ and the inclination of the dependence $D(t)$ towards larger MCSs, respectively, in Figs. 4—7), as well as the transition from the two- to three-stage process (nucleation, growth, and coalescence).

The behaviors of the average radius $\langle r \rangle$ and the average volume $\langle V \rangle$ of new-phase particles in the course of the phase decomposition process are demonstrated in Fig. 6. The time-variation of the concentration C in the alloy is shown in Fig. 7.

Figures 3–7 confirm our thesis about the dependence of the decomposition stage number on the magnitude of initial supersaturation. The results testify to that the higher is C_0, the faster the alloy relaxes to the equilibrium state and approaches the stage of coalescence and coagulation.

One can see that, for large values of C_0, the fast nucleation and slow following processes are observed. A similar behavior was observed in amorphous alloys and quickly tempered metallic glasses $Al_{88}Y_7Fe_5$, $Al_{92}Sm_8$, $Al_{85}Ni_5Y_{10}$, and $Al_{90}Ni_6Nd_4$ [2]. The process of transformation of metallic glasses into crystals is often consists of two stages: a plenty of fine-grained structures emerges quickly at the first stage, while the second one is characterized by the slow growth of those structures [1, 2]. In the course of the collective nucleation and decomposition in a metastable alloy, there is the opportunity for the alloy to exist in the state of incomplete decomposition, with the formation of a nanocrystalline structure made up of a large number of new-phase nuclei surrounded by the depleted phase. Therefore, the process of decomposition in a strongly defective supersaturated alloy with the nucleation of the new phase can run with some delay in the state of incomplete decomposition. Such a state can be observed as amorphous by x-ray diffraction analysis, if the radii of the new-phase nuclei are small.

The behavior of the concentration in the simulated alloy is not obvious *a priori*. Namely, the higher the initial value C_0, the lower is its asymptotic value and the more quickly the latter can be reached. In this case, the width of the distribution function $f(u)$ (the dispersion) in the space of relative dimensions is larger for higher values of initial supersaturation.

Such a scenario explains the change of the average radius in time for various initial concentrations. The higher the initial supersaturation (concentration), the larger is the average radius of the new phase nuclei and, correspondingly, the average volume (Fig. 6).

3.3. Coalescence and coagulation stage

The distribution functions, obtained in the course of evolution, made the numerical analysis, carried out according to the quantitative statistical characteristics, which are calculated by the formulas quoted above, eligible at the coalescence stage as well.

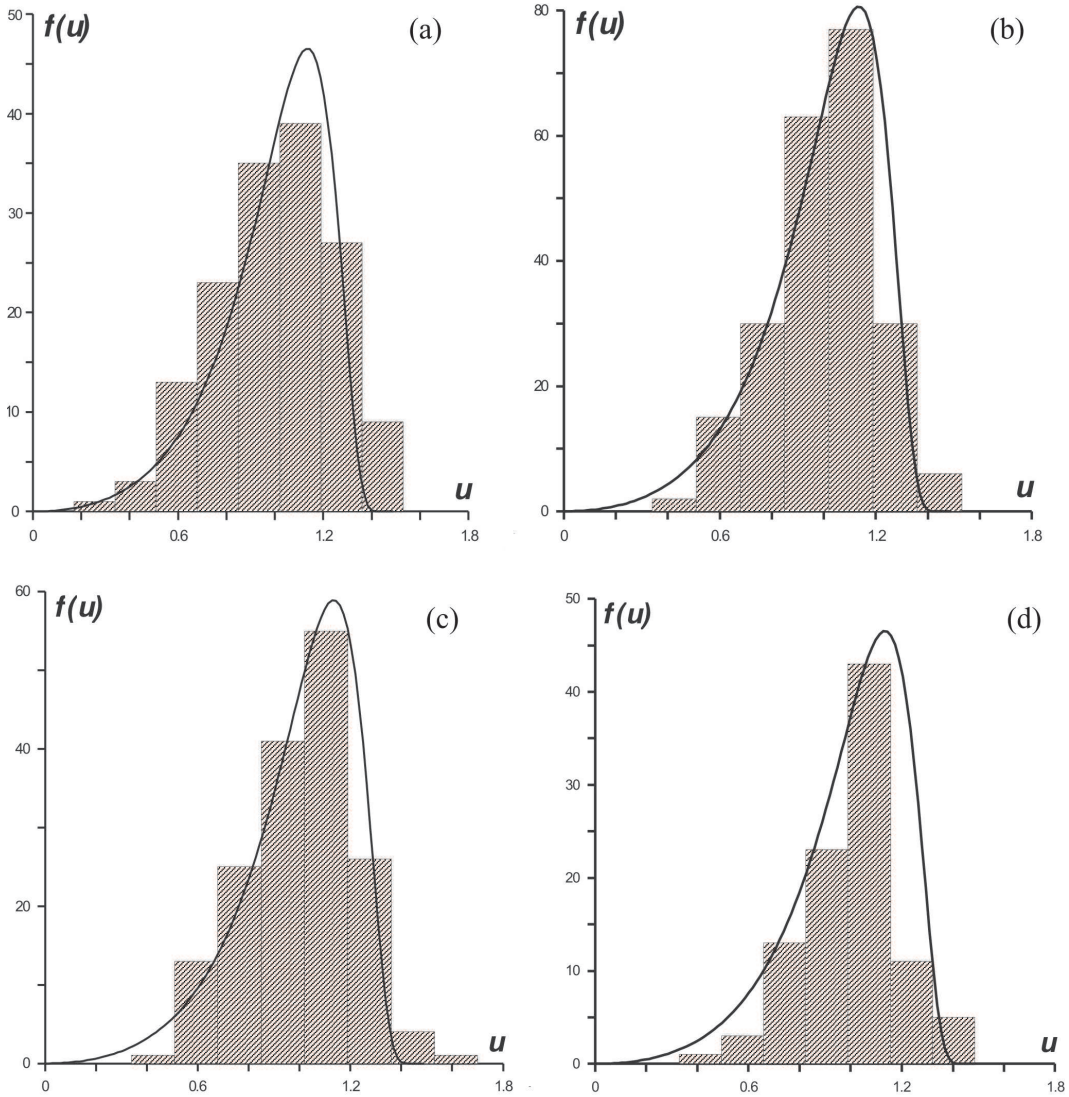

Fig. 8. Histograms of the distribution function of new-phase particles over their dimensions in the normalized space ($u = r/\langle r \rangle$) at the final stage of decomposition ($t = 8 \times 10^9$ MCS) for various values of $C_0 = 0.1$ (a), 0.075 (b), 0.05 (c), and 0.025 (d) and their comparison with the theoretical LSW curve obtained by formula (7) (solid curve)

At this stage, we have analyzed such characteristics as the average radius and the volume of the new-phase particles and the concentration in the parent phase during the phase decomposition. The results of the corresponding comparative analysis of the distribution function $f(u)$ obtained in the framework of our MC model with the results of the LSW theory are depicted in Fig. 8. Here, we monitored the evolution of the function $f(u)$ for various values of C_0.

The LSW theory brings about the universal function $f(u)$ describing the distributions of new-phase nuclei over the dimension, the asymptotic shape of which does not depend on the initial distribution. In this theory, the average size of aggregates $\langle r \rangle$ coincides with the critical radius $r_{\rm cr}$ for the running supersaturation, which varies in time, and increases following the asymptotic law $\langle r \rangle \sim t^{1/3}$. The total number of grains in a unit volume varies as $N \sim t^{-1}$, and the supersaturation drop as $\Delta C \sim t^{-1/3}$. Such a conclusion was also confirmed by the computer calculations carried out by the authors in the framework of the Fokker–Planck model, where atoms became attached to and detached from the new-phase nuclei following the continuous scheme of bonding monomers: $N-1 \leftrightarrow N \longleftrightarrow N+1$ [4]. As a consequence,

the well-known expression for the distribution function of nuclei over their dimensions was obtained.

According to the LSW theory, the function $f(u)$ at the stage of coalescence looks like [8]

$$f(u) = \begin{cases} \dfrac{3^4 e}{2^{5/3}} \dfrac{u^2 \exp[-1/(1-2u/3)]}{(u+3)^{7/3}(3/2-u)^{11/3}}, & u < \dfrac{3}{2}, \\ 0, & u \geq \dfrac{3}{2}. \end{cases} \quad (7)$$

It follows from the analysis of the results exposed in Fig. 8 that, at the final stage of decomposition, the parameters of the distribution function tend to the values which are close to those obtained in the framework of the LSW theory of coalescence. The comparison evidences for a qualitative similarity between our distribution function and that of the LSW theory. However, the more detailed analysis reveals the discrepancies in such characteristics as the sharpness, inclination, and dispersion of the peak, which increase as the initial supersaturation grows (see the table).

The fact that the linear approximations $\langle V \rangle \sim t^1$ and $V_{\text{tot}} \sim t^1$ cannot coincide with the temporal dependences of the LSW theory deserves attention. This is mostly connected with the fact that time in computer simulation is reckoned in MCS units and is not proportional to the actual time. Nevertheless, the approximations given enable one to estimate the tendencies of changes of the process parameters and their rates. The approximation $\langle r \rangle \sim t^n$ ($\langle V \rangle \sim t^m$) brings about the value of the exponential factor $n(m)$ within the limits from $n = 0.2$ ($m = 0.6$) for $C_0 = 0.1$ to $n = 0.15$ ($m = 0.54$) for $C_0 = 0.025$.

If more prolonged time intervals are analyzed, MC simulations reveal the simultaneous coalescence and coagulation. This results in a small number of the new-phase particles, so that plotting the distribution function over particle dimensions becomes inexpedient owing to poor relevant statistics.

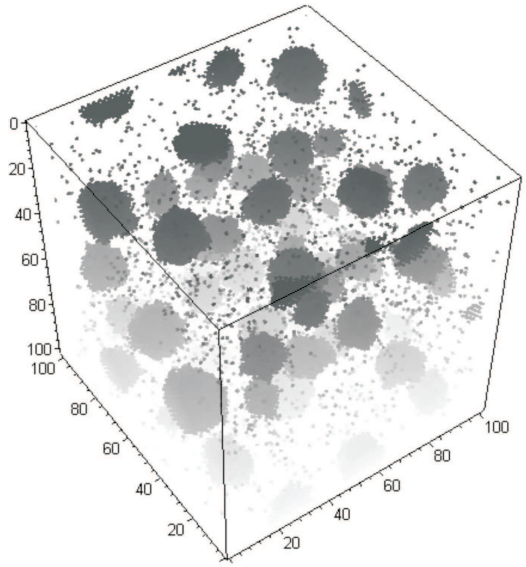

Fig. 9. Visualization of the new-phase particles in the 3D binary system at the final stage of the decomposition. The number of atoms equals 500000, $C_0 = 0.075$, and the number of MCSs equals 7500 (the Maple 9.0 program was applied). Isolated black dots correspond to the atoms of the sort B. Their large aggregations visualize the clusters of the new phase

3.4. Visual monitoring

As was said above, the model allowed all the results of calculations to be checked up visually with the help of the Maple 9.0 program. Figure 9 shows the example of such a verification.

4. Conclusions

A computer model of the vacancy diffusion has been developed on the basis of the MC method. An approach, which uses this model for studying the decomposition processes at the phase transitions of the first kind, has been proposed.

The kinetic analysis of the new phase nucleation, which accompanies the decomposition of a supersatura-

Dependence of the asymptotic, in time, values of the distribution function parameters on the initial concentration C_0

C_0	t, MCS	$\langle r \rangle$	$\langle V \rangle$	V_{tot}	D	Sk	Kr	N
LSW analytical model								
≈ 0	$\longrightarrow \infty$	$\sim t^{1/3}$	$\sim t^1$	const	0.215	−0.920	0.675	$\sim t^{-1}$
MC model								
0.1	8×10^9	$8.2(\sim 1.4 \times 10^{-10} t^1)$	$640(\sim 3.8 \times 10^{-8} t^1)$	$2.2 \times 10^{-14} t$	0.225	−0.06	−0.364	$98 + 4.8 \times 10^{11} t^{-1}$
0.075	8×10^9	$7.6(\sim 1.1 \times 10^{-10} t^1)$	$480(\sim 2.83 \times 10^{-8} t^1)$	$2.5 \times 10^{-14} t$	0.218	−0.28	0.046	$76 + 5.5 \times 10^{11} t^{-1}$
0.05	8×10^9	$6.9(\sim 1.2 \times 10^{-10} t^1)$	$360(\sim 2.33 \times 10^{-8} t^1)$	$3.5 \times 10^{-14} t$	0.204	−0.32	0.180	$78 + 4.4 \times 10^{11} t^{-1}$
0.025	8×10^9	$6.2(\sim 0.8 \times 10^{-10} t^1)$	$260(\sim 1.44 \times 10^{-8} t^1)$	$4.4 \times 10^{-14} t$	0.198	−0.55	0.577	$53 + 1.4 \times 10^{11} t^{-1}$

ted nanoalloy, has been carried out making use of the computer simulation method. The following graphical dependences have been plotted: the dependences of the average radius and the volume of the new-phase particles and the concentration in the parent phase on time; the distribution functions of nuclei over their dimensions at every stage of the phase separation process and for various initial concentrations; and the time evolution of the distribution function dispersion. The results of the computer experiments for various input parameters have been compared.

The numerical calculations testify to that the higher the initial supersaturation, the faster the alloy relaxes to the equilibrium state and the faster it approaches the coalescence one. An increase of the C_0 value for the simulated nanoalloy leads to the disappearance of the independent growth and interim stages. Such a conclusion brings us to the necessity of taking the interaction of the new-phase nuclei into account when considering the kinetics of the initial stages of the decomposition in nanoalloys with nonzero initial supersaturations [24, 25].

The MC model proposed in this work gave, at the final stage of the decomposition, the distribution of nuclei which is close to that of the LSW theory. The increase (decrease) of supersaturation resulted in the increase (decrease) of a discrepancy between our results obtained for the final stage of decomposition and those of the LSW theory.

The MC model demonstrated that, depending on the degree of initial supersaturation, the two- (for large supersaturations), three-, or even four-stage (for small supersaturations) processes of phase separation may occur.

The comparison of the characteristic times showed that, if the magnitude of C_0 is large, the nucleation stage is fast in comparison with the following ones. In the course of the collective nucleation and decomposition in a metastable alloy, there exists the opportunity for the alloy to be in the state of incomplete decomposition with the formation of a nanocrystalline structure composed of a large number of new-phase nuclei surrounded by a depleted phase. The two-stage behavior is observed in amorphous alloys and quickly quenched metallic glasses: at the first stage, a large number of fine-grained structures quickly appears; on the second, these structures slowly aggregate [1, 2].

The analysis carried out in this work is to be continued by the studies of the kinetics of the initial stages of the phase separation in a binary alloy, provided that several new phases can emerge, in case of the reaction diffusion in the binary diffusion pair. The simulation of a multicomponent system is also needed and planned to be done in the future.

The work was executed in the framework of the CRDF Program: CGP 2006-A, EMM Sciences, Proposal number 15484.

1. *Koster U.* // Ann. New York Acad. Sci. — 1986. — **484**. — P.45.
2. *Kelton K. F.* // Phil. Mag. Lett. — 1998. — **77**, N6. — P. 337 — 343.
3. *Slezov V.V. Schmelzer J.W.P.* // Nucleation Theory and Applications / Ed. by J.W.P. Schmelzer, G. Röpke, V.B. Priezzhev. — Dubna, Russia: JINR, 1999. — P. 6.
4. *Shirinyan A.S., Pasichny M. O.* // Visn. Cherkasy Derzh. Univ. Ser. Fiz. — 2002. — **36—37**. — P. 51—59.
5. *Lifshits I.M., Slezov V.V.* // Fiz. Tverd. Tela. — 1959. — **1**. — P. 1401 — 1410.
6. *Skripov V.P., Koverda V.P.* Spontaneous Crystallization of Supercooled Liquids. — Moscow: Nauka, 1984 (in Russian).
7. *Christian J.W.* The Theory of Transformations in Metals and Alloys. Part 1. Equilibrium and General Kinetic Theory. — Oxford: Pergamon Press, 1975.
8. *Lifshitz E.M., Pitaevskii L.P.* Physical Kinetics. — Oxford: Pergamon Press, 1981.
9. *Gusak A.M., Kovalchuk O.A.* // Phys. Rev. B. — 1998. — **58**, N 5. — P. 2551 — 2555.
10. *Kozubski R., Czekaj S., Kozlowski M. et al.* // 9-th Intern. Symp. on Physics of Materials ISPMA-9. — Praha, 2003.
11. *Fratzl P., Penrose O.* // Phys. Rev. B. — 1994. — **50**, N 5. — P. 3477—3480.
12. *Kovalchuk A.O.* Ph.D. thesis in physics and mathematics. — Cherkasy: Cherkasy Derzh. Univ., 2002.
13. *Pasichnyy M.O., Gusak A.M.* // Defect and Diffusion Forum. — 2005. — **237—240**. — P. 1193—1198 [http://www.scientific.net].
14. *Chuistov K.V.* Modulated Structure in Ageing Alloys. — Kyiv: Naukova Dumka, 1975 (in Russian).
15. *Trushin Yu.V.* Physical Materials Science. Kinetic theory of Metals. A Textbook. — St.-Petersburg: Nauka, 2000 (in Russian).
16. *Umanskii Ya.S., Skakov Yu.A.* Physics of Metals. — Moscow: Atomizdat, 1978 (in Russian).
17. *Krivoglaz M.A., Smirnov A.A.* Theory of Order-Disorder in Alloys. — London: MacDonald, 1969.
18. *Ziman J.M.* Principles of the Theory of Solids. — Cambridge: Cambridge University Press, 1964.
19. *Madelung O.* Introduction to Solid-State Theory. — Berlin: Springer, 1996.
20. *Kittel C.* Introduction to Solid State Physics. — New York: Wiley, 1995.

21. *Gusak A.M., Grytsenko V.G., Zaporozhets T.V.* Statistical Physics — Fundamentals and Models. — Cherkasy, 1998 (in Ukrainian).

22. *Jiang Yi, Glazier J.A.* // Phil. Mag. Lett. — 1996. — **74**, N2. — P. 119—128.

23. *Smirnov A.A.* Introduction to Solid State Physics. — Moscow: Nauka, 1978 (in Russian).

24. *Shirinyan A.S., Gusak A.M.* // Ukr. Fiz. Zh. — 1999. — **44**, N7. — P. 883—890.

25. *Shirinyan A.S., Gusak A.M., Desre P.J.* // J. Metastable and Nanocryst. Mater. — 2000. — **7**. — P. 17—40 [http://www.scientific.net/jmnm].

Received 16.03.05.
Translated from Ukrainian by O.I. Voitenko

3D-МОДЕЛЮВАННЯ МЕТОДОМ МОНТЕ-КАРЛО ПРОЦЕСУ РОЗПАДУ В БІНАРНОМУ СПЛАВІ

А.С. Ширінян, Ю.С. Білогородський

Р е з ю м е

Проведено детальний аналіз кінетики зародкоутворення нової фази в рамках тривимірного моделювання методом Монте-Карло в бінарному сплаві з ГЦК-ґраткою. Розраховано відповідні величини процесу, такі, як середній розмір частинок нової фази, кількість кластерів нової фази, об'єм, функцію розподілу частинок за розміром, дисперсію, пересичення в залежності від часу та параметрів системи. Застосоване наближення дозволяє значно покращити наше розуміння механізму зародкоутворення в системі, яка перебуває в метастабільному стані.